Journal of
Functional Biomaterials

MDPI

Article

MicroRNA-210 Enhances Cell Survival and Paracrine Potential for Cardiac Cell Therapy While Targeting Mitophagy

Rita Alonaizan [1,2,*], Ujang Purnama [1], Sophia Malandraki-Miller [1], Mala Gunadasa-Rohling [1], Andrew Lewis [1], Nicola Smart [1] and Carolyn Carr [1]

[1] Department of Physiology, Anatomy & Genetics, University of Oxford, Oxford OX1 3PT, UK; carolyn.carr@dpag.ox.ac.uk (C.C.)
[2] King Faisal Specialist Hospital & Research Centre, Riyadh 12713, Saudi Arabia
* Correspondence: rita.al-onaizan@hotmail.com or rita.alonaizan@dpag.ox.ac.uk

Abstract: The therapeutic potential of presumed cardiac progenitor cells (CPCs) in heart regeneration has garnered significant interest, yet clinical trials have revealed limited efficacy due to challenges in cell survival, retention, and expansion. Priming CPCs to survive the hostile hypoxic environment may be key to enhancing their regenerative capacity. We demonstrate that microRNA-210 (miR-210), known for its role in hypoxic adaptation, significantly improves CPC survival by inhibiting apoptosis through the downregulation of *Casp8ap2*, a ~40% reduction in caspase activity, and a ~90% decrease in DNA fragmentation. Contrary to the expected induction of Bnip3-dependent mitophagy by hypoxia, miR-210 did not upregulate *Bnip3*, indicating a distinct anti-apoptotic mechanism. Instead, miR-210 reduced markers of mitophagy and increased mitochondrial biogenesis and oxidative metabolism, suggesting a role in metabolic reprogramming. Furthermore, miR-210 enhanced the secretion of paracrine growth factors from CPCs, with a ~1.6-fold increase in the release of stem cell factor and of insulin growth factor 1, which promoted in vitro endothelial cell proliferation and cardiomyocyte survival. These findings elucidate the multifaceted role of miR-210 in CPC biology and its potential to enhance cell-based therapies for myocardial repair by promoting cell survival, metabolic adaptation, and paracrine signalling.

Keywords: heart regeneration; miR-210; cell therapy; cardiac progenitor cells; myocardial infarction; hypoxia; mitophagy; ischaemia

Academic Editors: Yuichi Matsuzaki and Ilia Fishbein

Received: 9 February 2025
Revised: 4 April 2025
Accepted: 16 April 2025
Published: 21 April 2025

Citation: Alonaizan, R.; Purnama, U.; Malandraki-Miller, S.; Gunadasa-Rohling, M.; Lewis, A.; Smart, N.; Carr, C. MicroRNA-210 Enhances Cell Survival and Paracrine Potential for Cardiac Cell Therapy While Targeting Mitophagy. *J. Funct. Biomater.* **2025**, *16*, 147. https://doi.org/10.3390/jfb16040147

1. Introduction

Clinical efforts to achieve heart regeneration have primarily concentrated on cell therapy, using mesenchymal stem cells, cardiomyocytes or cardiac-committed cells derived from pluripotent stem cells, and presumed cardiac progenitor cells (CPCs). Despite early promise from pre-clinical studies, the administration of these cell populations in clinical trials has shown limited beneficial effects. CPCs have demonstrated the ability to improve cardiac function in animal models of myocardial infarction (MI), despite lacking long-term retention and the ability to generate new cardiomyocytes. It is, therefore, believed that CPCs exert their therapeutic effects primarily in a paracrine fashion, releasing a multitude of bioactive molecules that influence the surrounding microenvironment and promote tissue repair [1].

CPCs can be isolated and expanded in culture via the formation of cardiospheres to give cardiosphere-derived cells (CDCs), by selecting specific markers such as Kit or Sca1 [1] or by expanding rare clonogenic cells [2], but this requires an extended period

to grow in culture, limiting their immediate clinical applicability as an autologous cell type. Clinical trials using intracoronary administration of autologous CDCs following MI showed a reduction in scar size [3]. Subsequent trials using allogeneic CDCs showed no change in scar size but improved segmental myocardial function post-MI [4] and improved left ventricular ejection fraction in patients with late-stage Duchenne muscular dystrophy [5]. Notable challenges associated with the use of CPCs are the long expansion time, cell death following transplantation, and low cell retention (reviewed in Alonaizan et al. 2022 [1]). Therefore, it is imperative to establish robust protocols that enable the time-effective expansion of CPCs and enhance their survival under ischaemia to fully harness their therapeutic potential in regenerative medicine.

We developed a collagenase/trypsin protocol adapted from studies by Gharaibeh et al. [6] and Okada et al. [7] for isolating slowly adhering cells (SACs) from skeletal muscle. These SACs demonstrated superior differentiation, survival, and therapeutic potential compared to rapidly adhering cells (RACs). When applied to cardiac tissue, the protocol produced a CPC population with more consistent cell yield and expansion time compared to CDCs, while maintaining a similar gene expression profile [8]. We have shown that these CPCs can be induced to differentiate into the cardiomyocyte lineage in vitro [9] using a TGFβ1-based protocol [10,11]. Additionally, we enhanced this differentiation efficiency by stimulating the PPARα pathway through fatty acid supplementation [9].

One critical factor that plays a pivotal role in enhancing the survival and function of transplanted cells is the cellular response to hypoxia. MicroRNA-210 (miR-210) is a key player in this process. Unique among other hypoxamiRs, miR-210 is consistently and robustly induced under hypoxic conditions, such as those encountered in ischaemic damage [12]. *Casp8ap2,* which encodes caspase 8-associated protein 2, has been shown to be a direct target of miR-210 and has been implicated in cell cycle regulation [13], transcriptional control [14], and the activation of caspase 8 during apoptosis [15]. HIF1α has been shown to induce BNIP3-dependent mitophagy as an adaptive metabolic response to hypoxia to increase cell survival [16], but it is not known whether miR-210 acts via this pathway. Upregulating miR-210 in cells before transplantation could significantly enhance their therapeutic efficacy. Therefore, understanding the mechanisms underlying miR-210 activation and exploiting them for therapeutic purposes holds immense promise. The primary aim of this research is to enhance cell retention after transplantation by utilising miR-210, paving the way for more effective cell-based therapies.

2. Materials and Methods

2.1. Mice

Male C57BL/6 mice aged 8–12 weeks (Harlan, Oxon, UK) were kept under a 12 h light–dark cycle, with controlled conditions of temperature and humidity and free access to water and chow. All animal procedures were reviewed and approved by the University of Oxford Animal Welfare and Ethical Review Board and conformed to the Animals (Scientific Procedures) Act of 1986, incorporating Directive 2010/63/EU of the European Parliament (PPL #3003322 approved 5 December 2017).

2.2. Isolation of Mouse CPCs

Mice were terminally anesthetised with isoflurane, and their hearts were isolated and rinsed with Dulbecco's phosphate-buffered saline (DPBS), containing 50 mg of primocin (an antimicrobial agent; InvivoGen, Toulouse, France). The atrial appendages were dissected and mechanically minced into small fragments (1–2 mm^3). These tissue pieces were then transferred into a digestion solution containing 0.1% trypsin and 0.1% Collagenase II (Calbiochem, 286 U/mg) in DPBS and incubated in a 37 °C water bath for a total of 40 min.

Every 10 min, the digestion mix was mechanically triturated by pipetting and allowed to settle on ice for 1 min, and the supernatant was collected. Fresh digestion solution was added to the remaining tissue for a total of four digestion cycles. During the final digestion step, the tissue was triturated with a sterile 19 G needle attached to a 1 mL syringe. After each digestion step, the collected supernatant was neutralised and the resulting cell suspension was resuspended in fresh complete explant medium (CEM) [17] before being passed through a 40 μm cell strainer and plated in a 12-well plate. The wells were pre-coated with fibronectin bovine plasma (2 μg/mL in DPBS; Sigma-Aldrich, Burlington, Massachusetts, USA) at a concentration of 50 μL per cm^2. The cells were then allowed to attach for three days without media changes.

2.3. Expansion of CPCs

Primary CPCs were cultured in CEM composed of IMDM (ThermoFisher, Waltham, MA, USA) supplemented with 20% FBS, 100 U/mL penicillin, 100 μg/mL streptomycin, and 2 mM L-glutamine (ThermoFisher) and plated on fibronectin-coated flasks.

2.4. Culture of HL-1 Cardiomyocytes

HL-1 cardiomyocytes [18] were maintained in Claycomb medium (Sigma-Aldrich); supplemented with 100 U/mL penicillin, 100 μg/mL streptomycin, 2 mM L-glutamine (ThermoFisher), 100 μM norepinephrine (Sigma-Aldrich) in 30 mM L-ascorbic acid (Sigma-Aldrich), and 10% FBS; and plated on flasks pre-coated with 0.02% (wt/vol) gelatin (Sigma-Aldrich) containing 5 μg/mL fibronectin.

2.5. Culture of HUVECs

Primary HUVECs, obtained from Lonza (Basel, Switzerland), were maintained in complete EGM-Plus (Cell Biologics, Chicago, IL, USA) supplemented with the provided supplement BulletKit: Endothelial Growth Supplement, L-glutamine, ascorbic acid, hydrocortisone hemisuccinate, human epidermal growth factor, heparin, gentamicin/amphotericin-B, and 2% FBS.

2.6. miRNA and siRNA Transfection Using DharmaFECT

Cells were seeded and allowed to attach overnight. DharmaFECT Transfection Reagent #1 (ThermoFisher) was used according to manufacturer's instructions. Briefly, miRNA or siRNA oligonucleotides and DharmaFECT were diluted in antibiotics/serum-free IMDM separately and incubated for 5 min at RT. The two solutions were then combined, mixed by gentle pipetting, and incubated for 20 min at RT before adding antibiotics-free CEM to the mix. The final concentration of oligonucleotides was 100 nM, unless otherwise indicated. Cells were incubated with the DharmaFECT/oligonucleotide solution for 48 h. The miRNAs and siRNAs used were the following: mmu-miR-210-3p mirVana miRNA mimic ID: MC10516 (#4464066), mirVana miRNA Mimic Negative Control (#4464059), Silencer Select Pre-Designed siRNA Application Silencer Select Assay ID: S63060 (#4390771), Silencer Select GAPDH Positive Control siRNA (#4390849), and Silencer Select Negative Control No. 2 siRNA (#4390846) (ThermoFisher).

2.7. Conditioned Media

CPCs transfected with miR-210, or negative miRNA as control, were cultured in serum-free IMDM for 48 h under normoxia or hypoxia. Conditioned media were collected for use in co-culture experiments (2.8) and for the assessment of release of growth factors (2.14).

2.8. Indirect Co-Culture of CPCs with HL-1 Cardiomyocytes and HUVECs

HUVECs were seeded at equal densities in 12-well plates, allowed to attach overnight in EGM-Plus media, and then subjected to serum starvation by switching to culture in 1:1 serum-free EGM-Plus media and CPC-conditioned media or -unconditioned media as a negative control for 24 h before harvesting for cell counting.

HL-1 cardiomyocytes were seeded at equal densities on gelatin-coated coverslips in 24-well plates, allowed to attach overnight in Claycomb media (Sigma-Aldrich), and then subjected to simulated ischaemia/reperfusion (I/R). This was performed by culturing the cardiomyocytes in serum- and glucose-free RPMI and hypoxia (1% O_2) for six hours to simulate ischaemia. HL-1 cardiomyocytes were then switched to culture under normoxia for 24 h to simulate reperfusion in 1:1 serum-free RPMI media and conditioned media or unconditioned media as a negative control. Apoptotic cell death was assessed using a TUNEL assay.

2.9. RNA Extraction and qRT-PCR

RNA was extracted from frozen cell pellets using the RNeasy Mini Kit (Qiagen, Hilden, Germany), and cDNA was synthesised using the High-Capacity cDNA Reverse Transcription kit (ThermoFisher) according to manufacturer's protocol. Real-time quantitative PCR was performed using the Applied Biosystems StepOnePlus Real-Time PCR System (Applied Biosystems, ThermoFisher). Relative mRNA levels were normalised to the housekeeping gene *Hprt*. SYBR Green fluorescent intercalating dye was used as a detection system for the reaction (SYBR Green PCR mastermix, ThermoFisher). For miR-210 qRT-PCR, RNA was extracted using miRNeasy Mini Kit (Qiagen) and cDNA was synthesised using miScript II RT Kit (ThermoFisher). Relative miR-210 levels were normalised to the housekeeping gene *Snord68* using the miR-210_2 and SNORD68_11 miScript Primer Assays. miScript SYBR Green PCR Kit (ThermoFisher) was used as a detection system for the reaction. The relative quantification of target gene expression was performed using the ΔΔCt Livak method [19], plotting the data as $2^{-\Delta\Delta Ct \pm SE}$. Primer sequences and information are provided in Table S1.

2.10. Quantifying Mitochondrial Copy Number by qPCR

DNA was extracted from cells using the DNeasy Blood & Tissue Kit (Qiagen), and SYBR Green fluorescent intercalating dye was used as a detection system for the reaction. The gDNA:mtDNA ratio was calculated by normalising the mitochondrial gene NADH dehydrogenase 1 (*mt-Nd1*) to the nuclear gene beta-2 microglobulin (*B2m*) using the ΔΔCt Livak method [19], plotting the data as $2^{-\Delta\Delta Ct \pm SE}$.

2.11. FAM-FLICA Poly Caspase Activity Assay

The FAM-FLICA Poly Caspase activity kit (Bio-Rad Laboratories, Hercules, CA, USA) measures apoptosis by detecting active caspases in cells via a cell-permeable reagent called the Fluorochrome Inhibitor of Caspases (FLICA), which comprises a caspase inhibitor sequence linked to a green (Carboxyfluorescein, FAM) fluorescent label. Cells were plated in Falcon 96-well black microplates with clear flat bottoms and allowed to reach 70–80% confluency. A 30X FAM-FLICA reagent was added at 1:30 after experimental manipulation of the plated cells, incubated for 45 min at 37 °C while mixing gently every 10 min, washed with media, and incubated for 60 min at 37 °C, thereby allowing unbound excess FLICA to diffuse out of the cells. Cells were washed with fresh media, and endpoint fluorescence was measured using an excitation wavelength of 488 nm and an emission filter of 530 nm on the Fluostar OPTIMA Microplate Reader (BMG Labtech, Ortenberg, Germany).

2.12. Terminal Deoxynucleotidyl Transferase dUTP Nick End Labelling Assay (TUNEL) Assay

The TUNEL assay was performed using Click-iT TUNEL Alexa Fluor 594 Imaging Assay (ThermoFisher), as per the manufacturer's instructions. DNase-I-treated slides were used for positive control. Samples were imaged using an Inverted Olympus FV1000 Confocal system. The percentage of cell apoptosis was determined by quantifying cells visualised in 3 random fields. Acquired images were processed using the Fiji software plugin JACoP [20].

2.13. MitoTracker Red CMXRos Staining

A working solution of 200 nM MitoTracker Red CMXRos (ThermoFisher), in basal IMDM, was added to the cells and incubated for 40 min. Cells were washed with DPBS and fixed with 4% PFA for 10 min at RT before staining with DAPI and being imaged using an Inverted Olympus FV1000 Confocal system at the excitation/emission wavelengths of 579/599 nm. Fluorescence intensity was quantified using Fiji software by assessing cells visualised in 3 random fields and measuring stained and background areas. Corrected total cell fluorescence (CTCF) was calculated using the following formula [21]:

$$\text{CTCF} = \text{integrated density} - (\text{area of selected cell} \times \text{mean fluorescence of background})$$

2.14. Growth Factor Array

The conditioned media were assessed by a C-Series Mouse Growth Factor Antibody Array Kit (RayBiotech, Peachtree Corners, GA, USA) that detects 20 growth factors, many of which had been implicated in cardiac repair. CPCs were transfected with either a negative miRNA or miR-210, then cultured under normoxia or hypoxia on fibronectin-coated plates in basal IMDM (as required by the manufacturer). Culture medium was collected after 48 h and stored at −80 °C. Before use, the culture medium was spun down to remove cell debris and was then run undiluted on the array following manufacturer's instructions. The arrays were imaged using a LI-COR scanner (LI-COR Biosciences, Cambridge, UK). The spots were analysed using a pixel counting programme (ImageStudioLite, Version 5.0) and the pixel counts normalised to the average of the positive control spots of each array.

2.15. ^{14}C Glucose Oxidation and ^{3}H Glycolysis Measurements

Glucose oxidation was measured using the method of Collins et al. [22], with some modifications as described in Malandraki-Miller et al. [9], which is dependent on the release of CO_2 during the passage of acetyl-CoA through the citric acid cycle. CPCs were seeded on fibronectin-coated 24-well plates, and the experimental treatment was carried out. Subsequently, CPCs were washed with DPBS then incubated for 3 h in no-glucose basal IMDM (ThermoFisher) supplemented with radiolabelled glucose at 12 mM containing 0.185 MBq D-U-^{14}C-glucose (PerkinElmer, Waltham, Massachusetts, USA). Wells with IMDM alone were assessed as negative controls, and wells without cells containing IMDM with ^{14}C-glucose were used to measure background radioactivity. The $^{14}CO_2$ produced by the glucose oxidation was trapped using 40% KOH-soaked filter papers placed in the wells of a 24-well plate used as a lid of the apparatus. A perforated rubber gasket, with holes corresponding to each well, separated the two plates. To ensure the system was sealed and avoid $^{14}CO_2$ leakage, the plates were wrapped tightly with Parafilm and screwed into a metal frame. Also, 70% perchloric acid was added to the wells to kill the cells and trigger the release of $^{14}CO_2$ after a 2 h incubation. It was injected through the top holes in the top plate, through the seal and into the well. The holes were instantly resealed with new parafilm. Subsequently, the samples were allowed to sit for 1 h to allow for the complete release of $^{14}CO_2$ that was dissolved in the media as $HCO^{-}{}_3$. The filter papers containing

trapped $^{14}CO_2$ were placed in scintillation vials filled with 10 mL of scintillation fluid (MP Biomedicals, Santa Ana, CA, USA) and analysed using the Tri-Carb 2800TR Liquid Scintillation Analyzer (PerkinElmer), which measured radiation counts per minute.

Glycolysis was measured as described in Malandraki-Miller et al. [9]. CPCs were incubated for 6 h in no-glucose basal IMDM supplemented with radiolabelled glucose at 12 mM, containing 0.118 MBq ^{3}H-glucose (PerkinElmer). Wells with IMDM alone were assessed as a negative control. Following incubation, the culture media contained both released ^3H_2O and remaining ^{3}H-glucose. Therefore, ^3H_2O was separated from ^{3}H-glucose using a Dowex 1 × 4 chloride form (Sigma-Aldrich) anion exchange column, which binds the ^{3}H-glucose and elutes ^3H_2O. To prepare the columns, 250 g of Dowex resin was added to a 1.25 M NaOH and 1.61 M boric acid solution and washed with distilled H_2O until the pH reached 7.5. The prepared solution was then added to glass Pasteur pipettes plugged with glass wool. Scintillation vials were filled with 10 mL of scintillation fluid (MP Biomedicals) and placed underneath the columns to collect the eluted samples. Subsequently, 200 µL of each culture medium sample was added to a column, allowing for the ^{3}H-glucose to bind to the column for 15 min before washing each column with 2 mL of distilled H_2O for ^3H_2O to be eluted into the scintillation vials. The samples were analysed using the Tri-Carb 2800TR Liquid Scintillation Analyzer (PerkinElmer), which measured radiation counts per minute.

2.16. Statistical Analysis

Results are presented as means ± standard deviations. All statistical analyses were performed using Graphpad Prism (Version 10.3.0). Data were analysed using unpaired two-tailed Student's *t*-tests where there were two data sets being compared (i.e., control and treated samples) or one-way analysis of variance (ANOVA) with a Tukey post hoc analysis for three or more data sets, unless otherwise indicated. Sample sizes are provided in the figure legends. Statistical significance was accepted at $p < 0.05$.

3. Results

3.1. miR-210 Improves the Survival of CPCs by Targeting Apoptotic Cell Death Following Serum Starvation

CPCs were isolated from mouse atria, expanded to passage 7, and then transfected with miR-210 or a negative-miRNA. miR-210 overexpression was confirmed 48 and 72 h after transfection using qRT-PCR (Figure S1). To validate miR-210's pro-survival effect and confirm that it targets cell death pathways in CPCs, the expression of its known direct target, *Casp8ap2* [23], was analysed after miRNA transfection and 72 h of serum starvation. *Casp8ap2* expression was significantly reduced following miR-210 transfection in comparison to the negative miRNA (Figure 1A). A poly-caspase activity assay revealed significantly reduced overall activity of caspases following miR-210 transfection in comparison to the negative miRNA (Figure 1B). Finally, reduced apoptotic cell death was confirmed by measuring DNA fragmentation using a TUNEL assay (Figure 1C,D).

3.2. Unlike Hypoxia, miR-210 Does Not Induce BNIP3 as an Anti-Apoptotic Mechanism

To examine a potential relationship between the hypoxamiR miR-210 and mitophagy-induced cytoprotection, we examined the expression of mitophagy-associated genes in response to hypoxic culture and/or miR-210 overexpression. We found that hypoxic culture increased the expression of *Bnip3*, *Nix*, and *Atg4c*, but not *Atg7*, indicating enhanced mitophagy (Figure S2).

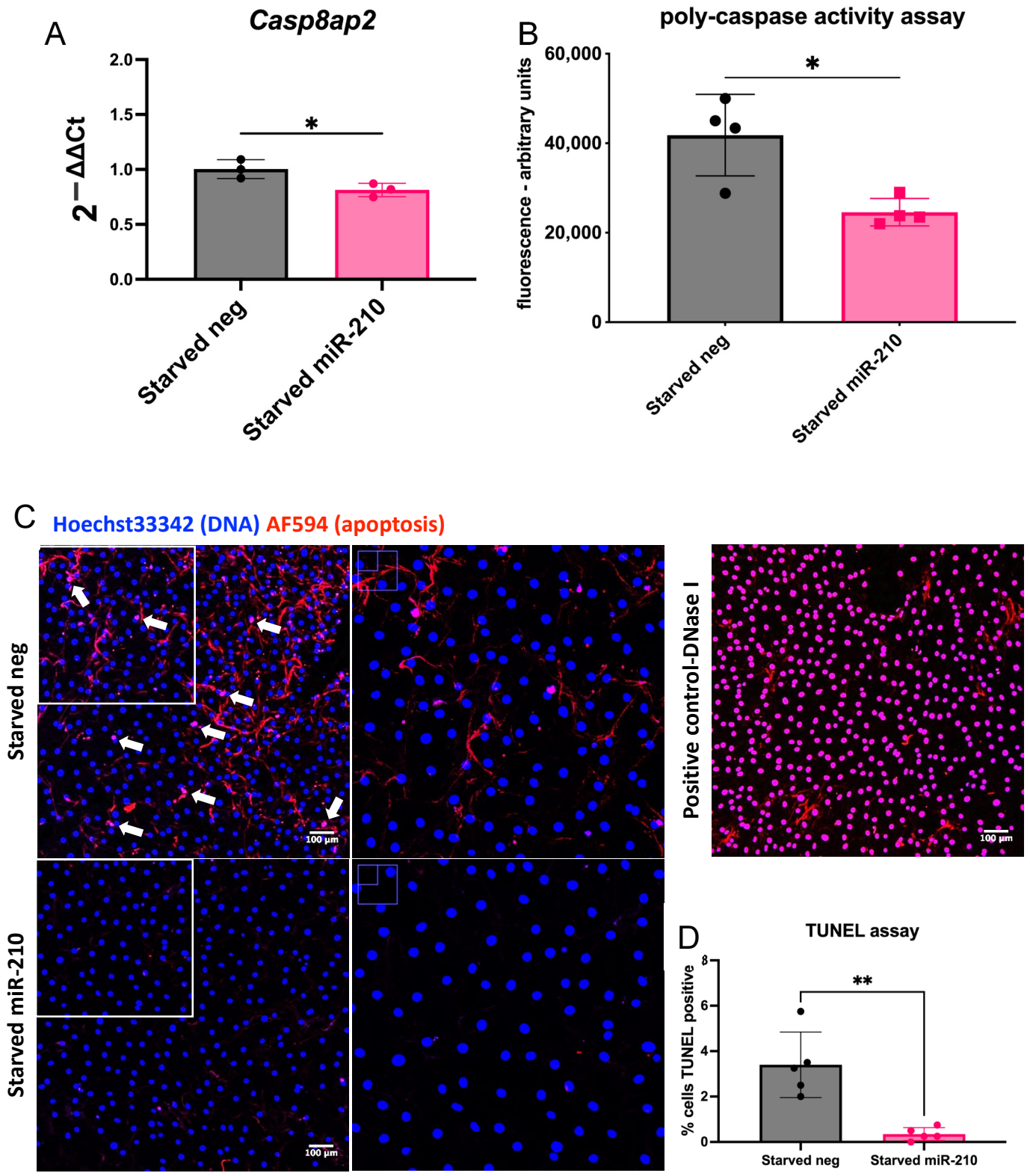

Figure 1. miR-210-transfected CPCs show decreased apoptosis following serum starvation. (**A**) *Casp8ap2* mRNA levels ($n = 3$) and (**B**) poly-caspase activity in miR-210-transfected CPCs following serum starvation, in comparison to CPCs transfected with a negative miRNA ($n = 4$). (**C**) DNA fragmentation represented as TUNEL$^+$ cells in miR-210-transfected CPCs following serum starvation, in comparison to CPCs transfected with a negative miRNA. Cells were imaged using an FV1000 confocal microscope. High-power inserts are shown by white boxes. DNase treatment was used as a TUNEL assay positive control; scale bar = 100 µm. (**D**) Quantification of the TUNEL assay ($n = 5$). Analysed using a *t*-test; * $p < 0.05$, ** $p < 0.01$.

To assess whether the cytoprotective role of miR-210 acted partly through BNIP3-dependent mitophagy, we knocked down the mRNA levels of *Bnip3* in CPCs using siRNA (Figure S3) and measured apoptosis following 72 h of serum starvation. *Bnip3* knockdown did not decrease miR-210's capacity to target apoptosis (Figure 2A,B). This suggests that unlike the previously described role of HIF1α [16], miR-210 does not induce BNIP3 as an anti-apoptotic mechanism. A significant reduction in apoptosis was still observed in miR-210-transfected cells in comparison to their respective negative miRNA group in both *Bnip3* siRNA and negative siRNA conditions, which is consistent with miR-210's pro-survival effect.

Bnip3 and *Nix* mRNA expression was measured in miR-210-overexpressing CPCs cultured under normoxia or hypoxia with or without serum starvation (Figure 2C). We found that miR-210 did not significantly alter *Bnip3* expression but reduced *Nix* expression in CPCs cultured in control conditions under hypoxia in comparison to their respective negative miRNA group. Interestingly, *Nix* and *Bnip3* expression was decreased in response to serum starvation under hypoxia. In contrast, an increase in *Nix* expression was observed in response to serum starvation under normoxia and no significant change was observed with *Bnip3*. Overall, this shows that, unlike hypoxia, miR-210 does not induce Bnip3-dependent mitophagy as an anti-apoptotic mechanism. In contrast, the reduction in *Nix* levels following the miR-210 transfection of CPCs under hypoxia suggested that there might, in fact, be a reduction in mitophagy levels. Therefore, this was further investigated.

3.3. Mitophagy as a Target of the Hypoxamir miR-210

Expression levels of *Pink1* were assessed as the PINK1-Parkin pathway is the most widely studied mode of mitophagy. We found that *Pink1* was significantly reduced in miR-210-overexpressing CPCs in comparison to their respective negative miRNA group under all conditions, except for the starved normoxic condition (Figure 3A). *Atg4c* expression was reduced in miR-210-overexpressing CPCs in comparison to their respective negative miRNA group in hypoxic conditions, whereas *Atg7* expression levels were not significantly altered. We also saw a decrease in the expression of the mitochondrial fission factor *Drp1* in miR-210 overexpressing CPCs in starved cells under normoxia and control cells under hypoxia. A significant increase in *Drp1* levels in response to serum starvation was observed in control and miR-210 over-expressing cells cultured under hypoxia.

Mitotracker CMXRos was used as a measure of mitochondrial membrane potential. We found an increase in Mitotracker CMXRos retention in miR-210-transfected CPCs in comparison to the negative miRNA groups in all groups, except control cells under hypoxia. In contrast, there was no significant change in response to serum starvation (Figure 3B,C). Mitochondrial copy number was also assessed by mitochondrial DNA/genomic DNA ratio using qRT-PCR. We observed increased mitochondrial copy number in miR-210-transfected CPCs in all conditions in comparison to their respective negative miRNA group (Figure 3D).

Mitophagy can act as a modulator of metabolism and cell fate [23]. Additionally, the degree of mitophagy has been shown to be dependent on the metabolic context [24]. We therefore examined the rates of glycolysis and glucose oxidation of miR-210-transfected CPCs to determine whether they were consistent with reduced mitophagy. As both measurements involved the use of radioactive material, they were performed in a radioactivity lab where only a normoxic incubator was available for use. We found a significant increase in glucose oxidation rates in control miR-210-transfected CPCs, in comparison to their respective negative miRNA group, but no change after serum starvation (Figure 3E). No significant changes in glycolysis were detected. Altogether, these results suggested reduced mitophagy in response to miR-210 overexpression.

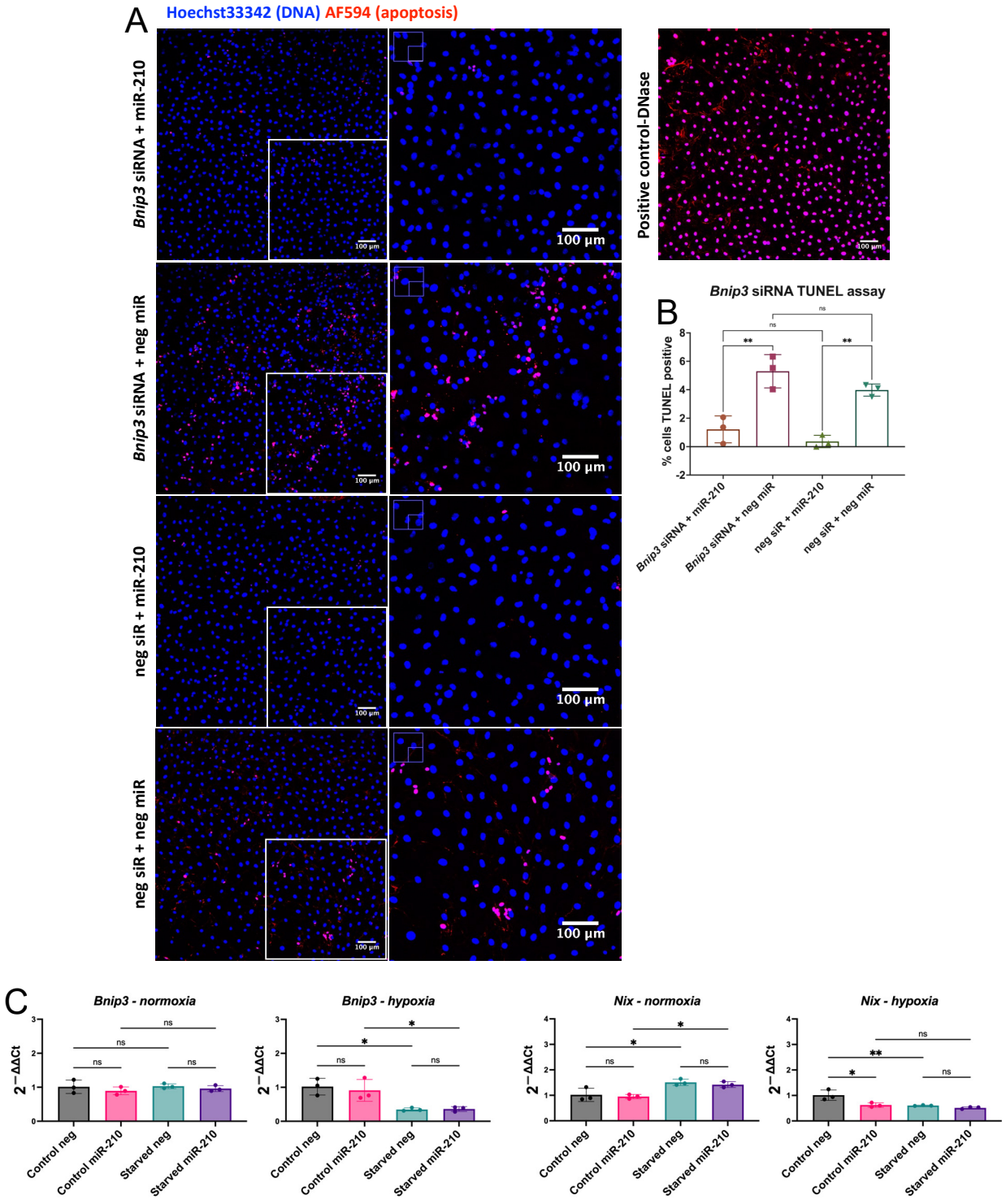

Figure 2. Cytoprotection in miR-210-transfected CPCs is not affected by *Bnip3* knockdown but miR-210 decreases expression of *Nix* in CPCs under hypoxia. (**A**) DNA fragmentation represented as TUNEL$^+$ cells following serum starvation of CPCs transfected with the following: (top to bottom) *Bnip3* siRNA + miR-210, *Bnip3* siRNA + negative miRNA, negative siRNA + miR-210, negative siRNA + negative miRNA. Cells were imaged using an FV1000 confocal microscope. High-power inserts (right column) are shown by white boxes. DNase treatment was used as a TUNEL assay positive control. (**B**) The quantification of the TUNEL assay. (**C**) mRNA levels of *Bnip3* and *Nix* in miR-210-transfected CPCs, in comparison to CPCs transfected with a negative miRNA, under the following conditions: control media and normoxia, serum starvation and normoxia, control media and hypoxia, serum starvation and hypoxia. Analysed using a one-way ANOVA with Tukey's multiple comparisons test ($n = 3$); ns = not statistically significant, * $p < 0.05$, ** $p < 0.01$.

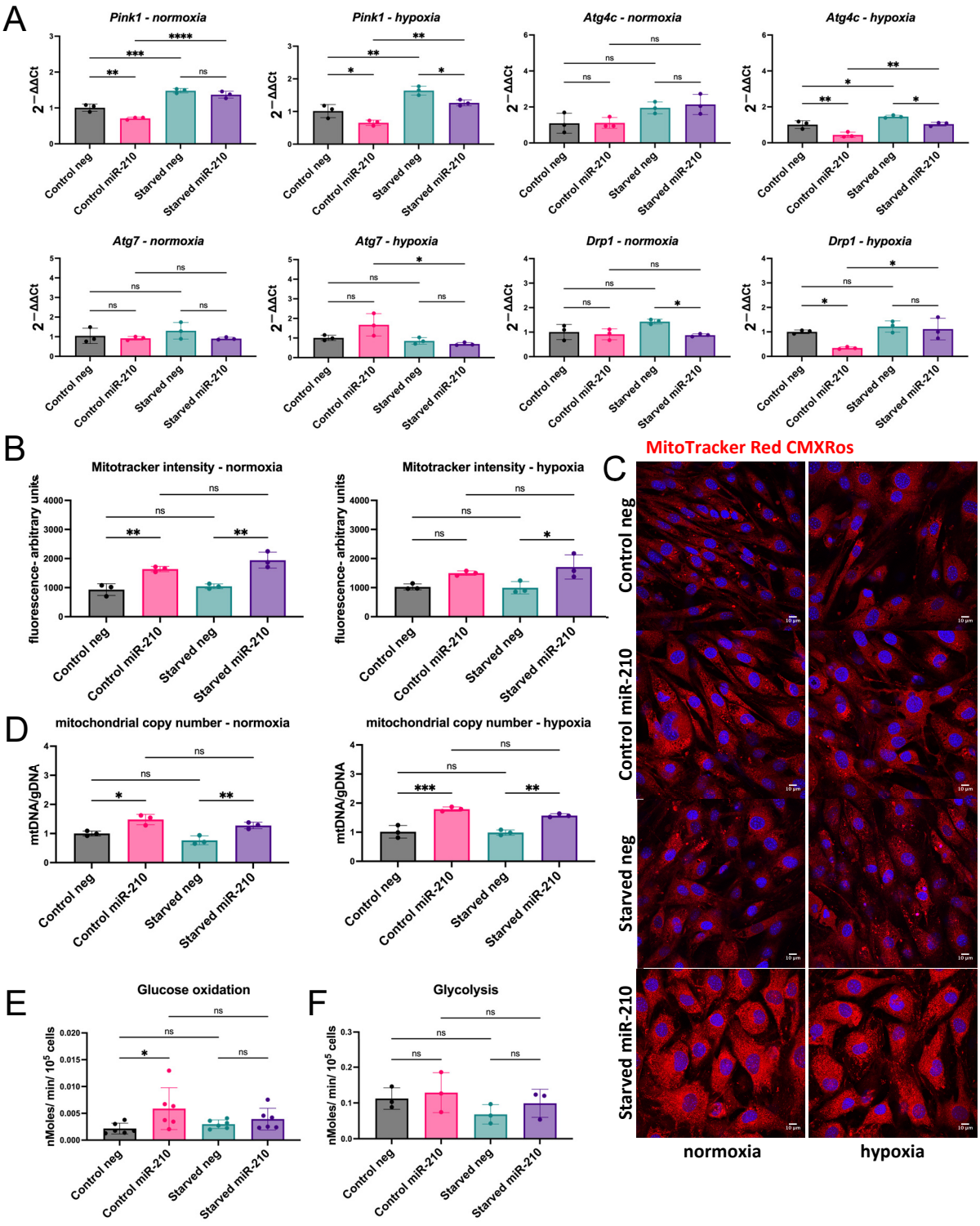

Figure 3. miR-210-transfected CPCs show decreased mitophagy and higher glucose oxidation levels. (**A**) mRNA levels of *Bnip3*, *Nix*, *Pink1*, *Atg4c*, *Atg7*, *and* the fission factor *Drp1* in miR-210-transfected CPCs in comparison to CPCs transfected with a negative miRNA, under the following conditions: control media and normoxia, serum starvation and normoxia, control media and hypoxia, serum starvation and hypoxia ($n = 3$); (**B**,**C**) Mitotracker intensity quantification and representative images ($n = 3$; scale bar = 10 µm); (**D**) mitochondrial copy number ($n = 3$); (**E**) glucose oxidation ($n = 6$) and (**F**) glycolytic ($n = 3$) rates measured as nMoles/min/10^5 cells, under the following conditions: control media and serum starvation. Analysed using a one-way ANOVA with Tukey's multiple comparisons test; ns = not statistically significant, * $p < 0.05$, ** $p < 0.01$, *** $p < 0.001$, **** $p < 0.0001$.

3.4. miR-210 Overexpression in CPCs Reveals a Complex Relationship with Hypoxia-Inducible Genes

miR-210 is regarded as a hypoxamiR that is capable of upregulating HIF1α via a positive feedback loop [25]. However, our results indicated that unlike HIF1α, miR-210 may have a role in reducing mitophagy and enhancing oxidative metabolism. This warranted us to further explore the relationship between miR-210 and HIF1α by assessing the effect of miR-210 on the expression of the known HIF1α target pyruvate dehydrogenase kinase 1 (*Pdk1*) [26,27] as well as targets by which miR-210 has been shown to induce hypoxic adaptations. For example, it has been shown that miR-210 targets *Iscu*, which encodes the mitochondrial iron sulphur scaffold protein, to induce a glycolytic shift in human cancer cell lines [28]. Moreover, we examined the mRNA levels of HIF1α stability regulators *Phd1* and *Phd3*.

We found that *Iscu1* expression was significantly reduced in miR-210-overexpressing CPCs in comparison to their respective negative miRNA group under all conditions. *Iscu2* expression was reduced in miR-210-overexpressing CPCs in comparison to their respective negative miRNA group in starved hypoxic conditions. Moreover, we observed an increase in *Iscu1* and *Iscu2* expression in almost all conditions in response to serum starvation (Figure 4). As we saw with miR-210 overexpression, hypoxic culture significantly decreased *Iscu1* and *Iscu2* levels (Figure S4).

The effect of miR-210 overexpression on *Pdk1*, *Phd1*, and *Phd3* was less consistent. *Pdk1* expression was reduced in miR-210-overexpressing CPCs in comparison to their respective negative miRNA group in control media under hypoxia but not in other conditions; *Phd1* was only reduced by miR-210 overexpression in CPCs in control media under normoxia; and *Phd3* was only reduced in starved media under normoxia. After serum starvation, we observed the increased expression of *Pdk1* and *Phd1* in miR-210-overexpressing CPCs under hypoxia and of *Phd3* expression in both control and miR-210-overexpressing CPCs under normoxia (Figure 4. Unlike miR-210 overexpression, hypoxic culture significantly increased *Pdk1* and *Phd3* expression (Figure S4). This revealed a complex relationship between the effect of the hypoxamiR miR-210 and that of hypoxia.

3.5. miR-210-Overexpressing CPCs Enhance HUVEC Proliferation and HL-1 Cardiomyocyte Survival Through Paracrine Mechanisms

Due to the significant implication of paracrine signalling in the therapeutic effect of cell therapy on heart remodelling and regeneration, we assessed the ability of miR-210 to increase the secretion of beneficial growth factors from CPCs cultured under normoxia or hypoxia for 48 h. When CPCs were transfected with miR-210, an increase in SCF, IGF-1, and IGFBP-2 secretion was observed compared to the negative groups under normoxia but not hypoxia (Figure 5A,B).

HUVECs were used to evaluate the paracrine potential of CPC-conditioned media and whether this was enhanced by miR-210 transfection. HUVECs were switched to culture in 1:1 serum-free HUVEC media, treated with conditioned media or unconditioned media as a negative control for 24 h, and then harvested for cell counting. Conditioned media of CPCs cultured under hypoxia, but not normoxia, enhanced the proliferation of HUVECs in comparison to the negative control. Moreover, conditioned media of normoxic, but not hypoxic, miR-210-overexpressing CPCs significantly enhanced the proliferation of HUVECs in comparison to that of CPCs transfected with the negative miRNA (Figure 5C).

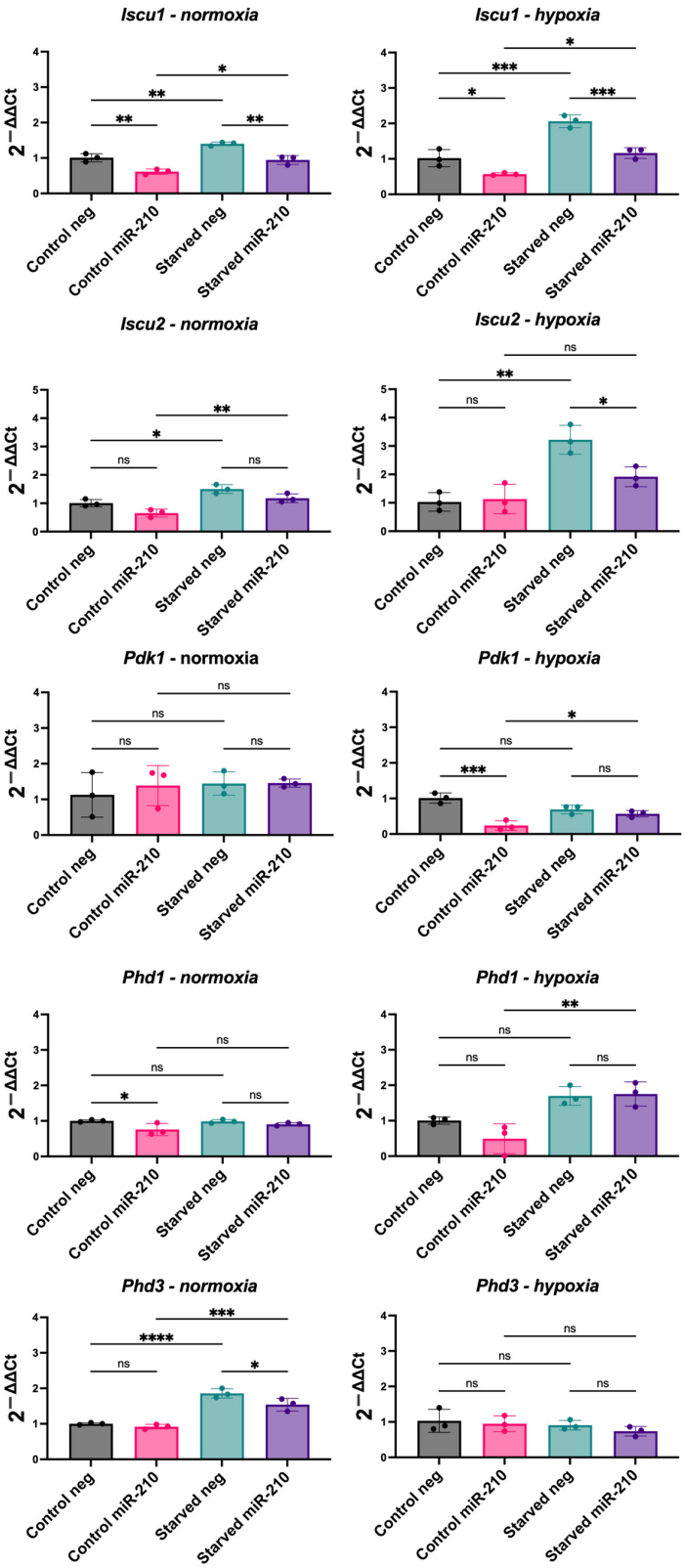

Figure 4. Expression of hypoxia-associated genes in miR-210-transfected CPCs cultured under normoxia or hypoxia, with or without serum starvation. mRNA levels of *Iscu1*, *Iscu2*, *Pdk1*, *Phd1*, and *Phd3* in miR-210-transfected CPCs, in comparison to CPCs transfected with a negative miRNA, under the following conditions: control media and normoxia, serum starvation and normoxia, control media and hypoxia, serum starvation and hypoxia. Analysed using a one-way ANOVA with Tukey's multiple comparisons test ($n = 3$; ns = not statistically significant, * $p < 0.05$, ** $p < 0.01$, *** $p < 0.001$, **** $p < 0.0001$).

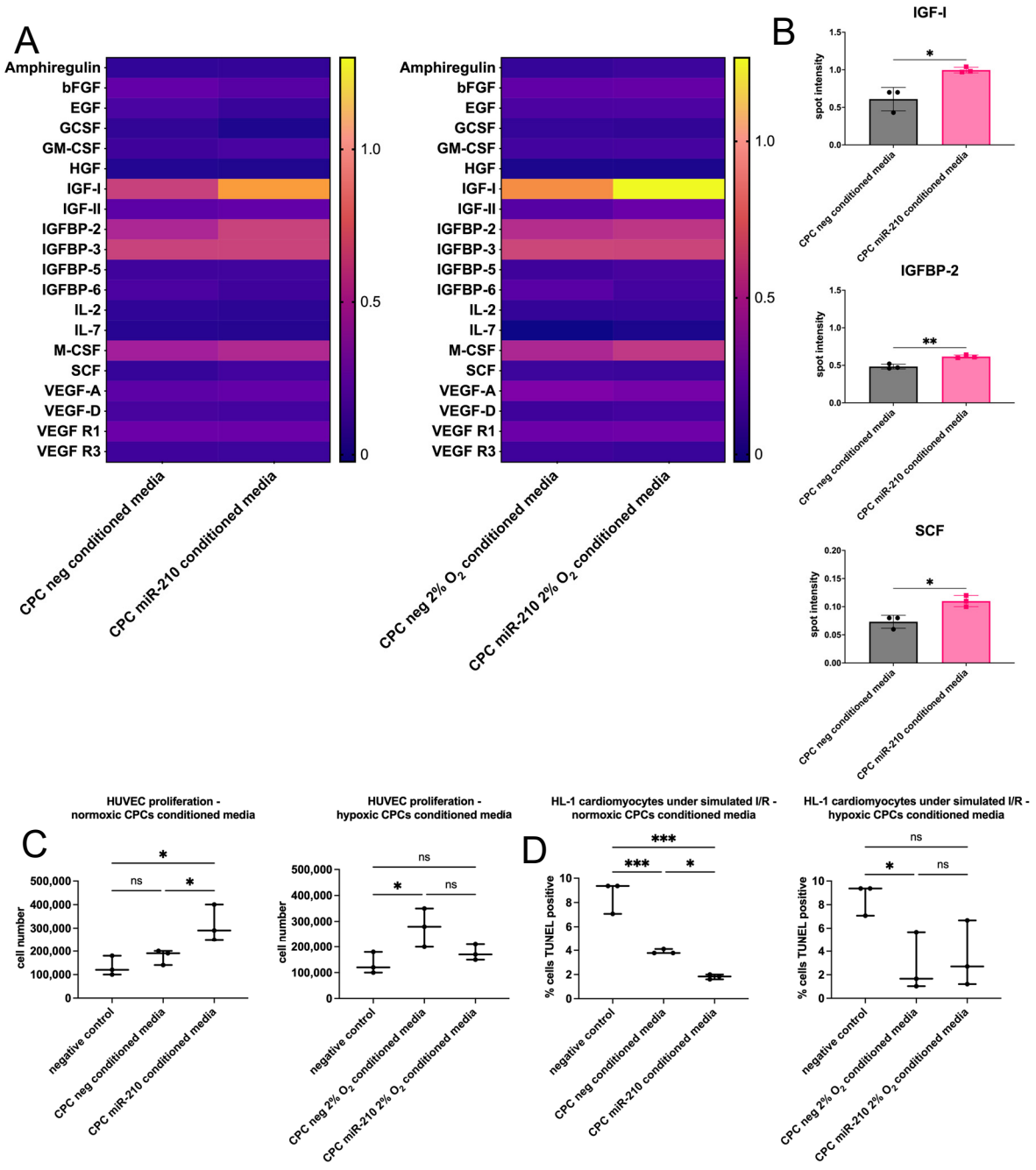

Figure 5. miR-210 enhances the paracrine potential of CPCs as shown by increased HUVEC proliferation and an anti-apoptotic effect in HL-1 cardiomyocytes during indirect co-culture. (**A**) The secretion of 20 growth factors was assessed using an array in the conditioned media of miR-210-transfected CPCs, in comparison to CPCs transfected with a negative miRNA, after 48 h culture under normoxia or hypoxia. Spot intensity of the samples was normalised to the average of the positive control spots of each array. The heatmap illustrates spot intensity (black is low or absent; yellow is high) of the assessed factors secreted from CPCs cultured in normoxia or hypoxia. (**B**) Individual representation of growth factors with significantly increased secretion in miR-210-transfected CPCs cultured under normoxia compared with controls. Analysed using a *t*-test ($n = 3$; * $p < 0.05$, ** $p < 0.01$). (**C**) HUVEC proliferation in 1:1 serum-free HUVEC media and (**D**) TUNEL$^+$ cells in HL-1 cardiomyocytes after 24 h culture with conditioned media of miR-210-transfected CPCs or of negative miRNA-transfected CPCs, with unconditioned media as a negative control, where the conditioned media were from CPCs that had been cultured under hypoxia or normoxia for 48 h. Analysed using a one-way ANOVA with Tukey's multiple comparisons test ($n = 3$; ns = not statistically significant, * $p < 0.05$, ** $p < 0.01$, *** $p < 0.001$).

We next examined miR-210's ability to enhance the pro-survival effect of CPC-conditioned media on cultured cardiomyocytes. HL-1 cardiomyocytes were subjected to simulated ischaemia/reperfusion (I/R). This was performed by culturing the cardiomyocytes in serum- and glucose-free media and hypoxia (1% O_2) for 6 h to simulate ischaemia, followed by culturing in conditioned media or unconditioned media as a negative control and normoxia for 24 h to simulate reperfusion. Conditioned media of CPCs cultured under both normoxia and hypoxia decreased cardiomyocyte apoptosis under simulated I/R in comparison to the negative control (Figure 5D). Moreover, conditioned media of normoxic miR-210-overexpressing CPCs further decreased cardiomyocyte apoptosis in comparison to those of CPCs transfected with the negative miRNA.

4. Discussion

4.1. miR-210 Inhibits Apoptotic Cell Death

Contradictory roles of miRNAs have been described in the literature [29–32]. This may be attributed to the cell type and its gene expression profile and cellular microenvironment. It may also be a result of regulatory loops by the miRNA's own targets, as an miRNA and its targets can form both feedback and feedforward loops [33,34]. Moreover, the ability to have multiple targets in various pathways is an miRNA characteristic, which may give them the potential to conduct different regulatory effects.

In this study, we showed that miR-210 has an anti-apoptotic effect in CPCs in vitro by assessing *Casp8ap2* expression, caspase activation, and DNA fragmentation. We found that serum-starved CPCs showed significantly decreased *Casp8ap2* mRNA levels, poly-caspase activity, and DNA fragmentation when transfected with miR-210 in comparison to the negative miRNA, thereby indicating reduced apoptosis and superior survival potential. Although a pro-apoptotic role for miR-210 via ROS induction has been described [35], miR-210 has been shown to inhibit apoptotic cell death by targeting *Casp8ap2* [36], *Ptp1b*, and *Dapk1* [37]. Moreover, miR-210 promoted cardiomyocyte proliferation and inhibited apoptosis by targeting *Apc*, which encodes a cell cycle inhibitor [38]. miR-210 has also been shown to be enriched in exosomes secreted by CDCs, and these exosomes have been shown to have a cytoprotective role [39]. Moreover, miR-210 is upregulated in KIT^+ cell-derived exosomes subjected to hypoxia. These hypoxic exosomes improved cardiac function in a rat model of cardiac injury [40].

4.2. miR-210 Has a Role in the Regulation of Mitochondrial Fission and Autophagy

A role for miR-210 in mitophagy has not been previously explored. However, our results showing decreased *Nix*, *Pink1*, and *Drp1* levels and upregulated mitochondrial copy number and MitoTracker Red CMXRos retention in miR-210-transfected CPCs support a role for miR-210 in mitophagy. A study in endothelial progenitor cells revealed that transfecting the progenitors with miR-210 enriched for miR-210 in their secreted exosomes [41]. Treatment with these exosomes of endothelial cells subjected to I/R injury increased ATP levels and mitochondrial membrane potential and decreased mitochondrial fission [41]. This raises the question of whether mitophagy is a direct or indirect target of miR-210. A study reported that fibroblasts lacking caspases 3 and 7 are resistant to the loss of mitochondrial membrane potential [42]. Therefore, it can be argued that miR-210-induced caspase inhibition may be upstream of mitochondrial events. However, in our study, the reduction in mitophagy in miR-210-transfected CPCs was not confined to conditions of serum starvation, where caspase activation was higher than control conditions.

Mitophagy has been classically viewed as a mitochondrial quality control mechanism, but multiple reasons for mitochondrial elimination have been described. This is supported by observations ranging from programmed forms of mitophagy to basal mitophagy in dif-

ferent tissues, demonstrating the complex and multi-factorial nature of mitophagy [43]. The levels of basal activation are heterogenous across tissues and across different cells within the same tissue, highlighting context-dependant regulation that is not yet understood [24]. Indeed, it has been shown that levels of basal mitophagy depend on the metabolic context of the cell where greater levels are observed in highly metabolic cells such as cardiomyocytes and dopaminergic neurons [24]. Therefore, the observed downregulation in mitophagy is not necessarily linked to the pro-survival role of miR-210 in CPCs.

Moreover, programmed mitophagy describes instances where mitochondria are eliminated for developmental, physiological, or metabolic purposes [44]. Cell fate determination and differentiation often involve metabolic reprogramming that implicate mitophagy. A requirement for mitophagy to eliminate mitochondria is observed during the reprogramming of somatic cells into pluripotent stem cells that are highly glycolytic [45–47]. In this study, we observed an increase in glucose oxidation in miR-210-transfected CPCs cultured in control conditions under normoxia concordant with reduced mitophagy. These results, in addition to the previous data, further support the notion that the observed downregulation in mitophagy is not necessarily linked to the pro-survival role of miR-210 and may be a distinct function to induce a metabolic switch.

It remains ambiguous why a hypoxia-inducible miRNA would upregulate mitochondrial networks when the lack of oxygen would stimulate a HIF1α-induced metabolic switch to upregulate glycolysis and mitophagy [16,43]. Studies have reported that miR-210 has a negative effect on mitochondrial respiration with direct targets including *Iscu1/2* and *Cox10*, which are important factors in the mitochondrial electron transport chain [48–51]. Indeed, we found a downregulation in *Iscu1/2* mRNA levels in miR-210-transfected CPCs, as was also observed in CPCs cultured under hypoxia. However, when we examined *Pdk1* and *Phd1/3,* we found opposing effects of miR-210 transfection and hypoxic culture on their mRNA levels. PHDs are oxygen sensors that use oxygen as a co-substrate to induce the hydroxylation of HIF1α and subsequent polyubiquitination and proteasomal degradation [52]. Hypoxia, in turn, induces PHDs to allow for rapid HIF1α degradation upon reoxygenation [53–55]. Moreover, HIF1α upregulates PDK1 to inactivate pyruvate dehydrogenase, thereby blocking the entry of pyruvate into the mitochondria for oxidative phosphorylation [54]. In contrast, we saw a decrease in *Pdk1* and an increase in glucose oxidation, in miR-210-overexpressing CPCs under normoxia. Lethal forms of mitophagy have been described, for example, ceramide mediates caspase-independent cell death via excessive activation of mitophagy [56]. Therefore, miR-210 may be downregulating mitophagy to protect against lethality of excessive mitophagy that may occur in hypoxic environments.

Changes observed as a result of serum starvation include a consistent increase in *Iscu1/2* mRNA levels and an increase in *Pdk1*, *Phd1*, and *Phd3* in some conditions. These observed changes in response to serum starvation are contradictory, as both components involved in inducing a hypoxic phenotype (*Pdk1*) and others involved in inducing oxidative metabolism (*Iscu1/2*) are upregulated. Moreover, the upregulation in *Phd1/3* mRNA levels following serum starvation is similar to that observed following hypoxic culture. These changes do not appear to be differentially modulated in different conditions (i.e., neg- vs. miR-210-transfected CPCs or CPCs under normoxia vs. hypoxia). It is unclear why these various components would be upregulated following serum starvation, although this may explain why no significant changes were observed in the metabolic rates of CPCs following serum starvation. It has been previously shown that serum starvation alone induces mitochondrial fission [57], whereas eliminating glutamine or amino acids induces mitochondrial fusion, suggesting that starvation conditions can differentially affect mitochondrial fission and fusion [58]. Moreover, human fibroblasts subjected to serum starvation showed a continuous decrease in cellular ATP levels [59]. Serum starvation has been shown to in-

duce HIF1α as a pro-survival factor, even in normoxic cells [60,61]. All these reports are consistent with enhanced mitophagy and increased *Pdk1* and *Phd1/3* expression, although they contradict the observed increase in *Iscu1/2* mRNA levels. The contradictory effects of serum starvation may explain why the benefits of miR-210 transfection were more apparent in control conditions as opposed to starved conditions.

We examined the effect of miR-210 overexpression on *Bnip3* and *Nix* as they are both direct targets of HIF1α [62,63]. BNIP3 has been reported to induce apoptosis, necrosis, or autophagy depending on the cellular context [64]. The cytoprotective role of BNIP3-dependent mitophagy has been demonstrated in human primary epidermal keratinocytes [65]. Interestingly, *Nix* expression was increased in response to serum starvation under normoxia, but both *Nix* and *Bnip3* expression showed an opposite direction of change following serum starvation under hypoxia. BNIP3 and NIX share high sequence similarity, and identical functionality has been described. They are therefore expected to follow the same pattern. Both genes are induced by HIF1α [62,63], but their expression needs to be tightly regulated as over expression induces cell death [66]. Hypoxic culture increased *Bnip3* and *Nix* mRNA levels and showed a cytoprotective role in CPCs. Therefore, the opposite direction of change in *Bnip3* and *Nix* mRNA levels following serum starvation under hypoxia in comparison to normoxia may be a mechanism by which hypoxia fine-tunes their levels to protect against cell death.

Overall, our results demonstrated a pro-survival role for miR-210 in CPCs by showing that it reduced apoptosis following serum starvation. Our results also indicated a role for miR-210 in downregulating mitophagy, which is contrary to hypoxia but may be a mechanism by which miR-210 induces a metabolic shift and/or protects against lethality of excessive mitophagy in hypoxia. Whether or not the induced upregulation in mitochondrial dynamics by miR-210 is beneficial to the survival potential of transplanted CPCs in ischaemic heart tissue may be revealed by in vivo cell survival and retention studies. miR-210-transfected MSCs showed enhanced engraftment at four days after transplantation in infarcted rat hearts [67]. Moreover, we found that miR-210 reduced the expression of its known direct targets, *Iscu1/2*, which are also downregulated in hypoxia. This may be an indication of the capability of miRNAs to conduct different regulatory functions due to their ability to have multiple targets in various pathways. Our findings therefore highlight that the relationship between miR-210, HIF1α, and hypoxia is not as straightforward as once thought and warrants further investigation.

4.3. miR-210 Enhances Cell Paracrine Potential

miR-210 improved CPC paracrine function by increasing SCF, IGF-1, and IGFBP-2 secretion. SCF is a direct target of HIF1 and HIF2 and has been implicated in angiogenesis [68–71]. The cardiomyocyte-specific overexpression of SCF decreased myocardial apoptosis and improved cardiac function following MI [72]. Both IGF-1 and IGFBP-2 have been implicated in promoting angiogenesis [73]. IGF-1 has also been shown to have a cytoprotective effect in the infarcted heart [74]. This is concordant with the angiogenic effect of miR-210. The injection of an miR-210 vector into infarcted mouse hearts increased capillary density [37], and miR-210 has been demonstrated to target and repress *Efna3*, which encodes an inhibitor of angiogenesis [75]. *Efna3* repression by miR-210 in HUVECs is essential for the initiation of HUVEC tubulogenesis, revealing its vital role in angiogenesis [75]. Moreover, miR-210 overexpression in HUVECs stimulated cell migration and tubulogenesis, possibly through a Notch-dependant mechanism [76]. Our results show that miR-210 may have a role in regulating angiogenesis and/or cell survival by targeting IGF and SCF signalling. We observed an increase in the proliferation of HUVECs following incubation in the conditioned media of CPCs cultured under hypoxia, but not normoxia,

compared to the negative control. This is similar to the effect of CDC-conditioned media on HUVEC tubulogenesis [77] and studies reporting increased angiogenic paracrine signalling following hypoxic preconditioning of a variety of cell types [78–81].

Moreover, conditioned media of normoxic miR-210-overexpressing CPCs enhanced the proliferation of HUVECs in comparison to those of CPCs transfected with the negative miRNA, which may also be explained by an increase in the levels of pro-survival factors in the secretome of miR-210-transfected CPCs. We found that conditioned media of CPCs cultured under both normoxia and hypoxia decreased cardiomyocyte apoptosis under simulated I/R in comparison to the negative control. Likewise, a cytoprotective role of $SCA1^+$ cell-conditioned media has been demonstrated following hypoxic injury in HL-1 cardiomyocytes [82]. Moreover, we found that the conditioned media of normoxic miR-210-overexpressing CPCs further decreased cardiomyocyte apoptosis in comparison to those of CPCs transfected with the negative miRNA. miR-210 has been shown to transfer to primary neonatal cardiomyocytes co-cultured with MSCs via Cx43 gap junctions, resulting in the reduced expression of its pro-apoptotic target *Casp8ap2* and improved survival [67]. Moreover, the injection of an miR-210 vector into infarcted mouse hearts reduced the percentage of $TUNEL^+$ cardiomyocytes [37]. This observation may therefore be due to the secretion of miR-210 itself or the effect of other proteins or genetic material that may have been upregulated in the CPC secretome.

Overall, our findings support an anti-apoptotic role for miR-210 in cell therapy, though further in vivo studies are needed to confirm whether this is sufficient to enhance cell retention. We also propose a novel function for miR-210 in reducing mitochondrial autophagy, an unexpected role for a hypoxamiR. However, its connection to cell survival remains unclear and may instead indicate a role in metabolic reprogramming. Therefore, our study underscores the need to further investigate the interplay between miR-210 and hypoxia, as miR-210 does not consistently behave as a typical hypoxia-induced miRNA. Understanding whether miR-210-driven changes in mitochondrial dynamics increase the survival of transplanted cells in ischaemic heart tissue requires further research using in vivo models of ischaemia. Finally, we show that miR-210 enhances CPC paracrine function, reinforcing its potential as a conditioning agent for cardiac cell therapy. In conclusion, this study provides insights into the use of miR-210 to enhance the therapeutic potential of cell populations for transplantation following cardiac injury and the relationship between miR-210 and mitophagy that opens the door for further studies to uncover the behaviour of miR-210 as a hypoxia miRNA.

Supplementary Materials: The following supporting information can be downloaded at https://www.mdpi.com/article/10.3390/jfb16040147/s1, Figure S1: Confirmation of miR-210 overexpression after transfection in CPCs; Figure S2: Hypoxic culture upregulates the mRNA levels of mitophagy-associated genes in CPCs; Figure S3: Validation of *Bnip3* siRNA. Figure S4. Expression of mitophagy- and hypoxia-associated genes in CPCs cultured in hypoxia; Table S1: qRT-PCR primers. References [83–89] appear in the Supplementary Materials.

Author Contributions: Conceptualisation, R.A., N.S. and C.C.; formal analysis, R.A.; investigation, R.A., U.P., S.M.-M., M.G.-R. and A.L.; resources, C.C.; data curation, R.A.; writing—original draft preparation, R.A.; writing—review and editing, R.A., N.S. and C.C.; supervision, N.S. and C.C.; funding acquisition, R.A. All authors have read and agreed to the published version of the manuscript.

Funding: This research was funded by the King Faisal Specialist Hospital & Research Centre (PhD scholarship to R.A.).

Institutional Review Board Statement: The animal study protocol was approved by the University of Oxford Animal Welfare and Ethical Review Board and conformed to the Animals (Scientific

Procedures) Act of 1986, incorporating Directive 2010/63/EU of the European Parliament (PPL #3003322 approved 5 December 2017).

Informed Consent Statement: Not applicable.

Data Availability Statement: The raw data supporting the conclusions of this article will be made available by the corresponding author on request.

Conflicts of Interest: The authors declare no conflict of interest.

Abbreviations

CDCs	Cardiosphere-derived cells
CEM	Complete explant medium
CPCs	Cardiac progenitor cells
I/R	Ischaemia/reperfusion
MI	Myocardial infarction
miR-210	microRNA-210
RACs	Rapidly adhering cells
SACs	Slowly adhering cells

References

1. Alonaizan, R.; Carr, C. Cardiac regeneration following myocardial infarction: The need for regeneration and a review of cardiac stromal cell populations used for transplantation. *Biochem. Soc. Trans.* **2022**, *50*, 269–281. [CrossRef] [PubMed]
2. Noseda, M.; Harada, M.; McSweeney, S.; Leja, T.; Belian, E.; Stuckey, D.J.; Abreu Paiva, M.S.; Habib, J.; Macaulay, I.; de Smith, A.J.; et al. PDGFRalpha demarcates the cardiogenic clonogenic Sca1+ stem/progenitor cell in adult murine myocardium. *Nat. Commun.* **2015**, *6*, 6930. [CrossRef] [PubMed]
3. Malliaras, K.; Makkar, R.R.; Smith, R.R.; Cheng, K.; Wu, E.; Bonow, R.O.; Marban, L.; Mendizabal, A.; Cingolani, E.; Johnston, P.V.; et al. Intracoronary cardiosphere-derived cells after myocardial infarction: Evidence of therapeutic regeneration in the final 1-year results of the CADUCEUS trial (CArdiosphere-Derived aUtologous stem CElls to reverse ventricULar dySfunction). *J. Am. Coll Cardiol.* **2014**, *63*, 110–122. [CrossRef] [PubMed]
4. Ostovaneh, M.R.; Makkar, R.R.; Ambale-Venkatesh, B.; Ascheim, D.; Chakravarty, T.; Henry, T.D.; Kowalchuk, G.; Aguirre, F.V.; Kereiakes, D.J.; Povsic, T.J.; et al. Effect of cardiosphere-derived cells on segmental myocardial function after myocardial infarction: ALLSTAR randomised clinical trial. *Open. Heart* **2021**, *8*, e001614. [CrossRef]
5. McDonald, C.M.; Marban, E.; Hendrix, S.; Hogan, N.; Ruckdeschel Smith, R.; Eagle, M.; Finkel, R.S.; Tian, C.; Janas, J.; Harmelink, M.M.; et al. Repeated intravenous cardiosphere-derived cell therapy in late-stage Duchenne muscular dystrophy (HOPE-2): A multicentre, randomised, double-blind, placebo-controlled, phase 2 trial. *Lancet* **2022**, *399*, 1049–1058. [CrossRef]
6. Gharaibeh, B.; Lu, A.; Tebbets, J.; Zheng, B.; Feduska, J.; Crisan, M.; Peault, B.; Cummins, J.; Huard, J. Isolation of a slowly adhering cell fraction containing stem cells from murine skeletal muscle by the preplate technique. *Nat. Protoc.* **2008**, *3*, 1501–1509. [CrossRef]
7. Okada, M.; Payne, T.R.; Drowley, L.; Jankowski, R.J.; Momoi, N.; Beckman, S.; Chen, W.C.; Keller, B.B.; Tobita, K.; Huard, J. Human skeletal muscle cells with a slow adhesion rate after isolation and an enhanced stress resistance improve function of ischemic hearts. *Mol. Ther.* **2012**, *20*, 138–145. [CrossRef]
8. Alonaizan, R.; Chaves-Guerrero, P.; Samari, S.; Noseda, M.; Smart, N.; Carr, C. Transcriptomic analysis of adult mouse cardiac stromal cells using single-cell qRT-PCR. *bioRxiv* **2024**, 2024.2012.2022.629898. [CrossRef]
9. Malandraki-Miller, S.; Lopez, C.A.; Alonaizan, R.; Purnama, U.; Perbellini, F.; Pakzad, K.; Carr, C.A. Metabolic flux analyses to assess the differentiation of adult cardiac progenitors after fatty acid supplementation. *Stem. Cell Res.* **2019**, *38*, 101458. [CrossRef]
10. Smits, A.M.; van Vliet, P.; Metz, C.H.; Korfage, T.; Sluijter, J.P.; Doevendans, P.A.; Goumans, M.J. Human cardiomyocyte progenitor cells differentiate into functional mature cardiomyocytes: An in vitro model for studying human cardiac physiology and pathophysiology. *Nat. Protoc.* **2009**, *4*, 232–243. [CrossRef]
11. Goumans, M.J.; de Boer, T.P.; Smits, A.M.; van Laake, L.W.; van Vliet, P.; Metz, C.H.; Korfage, T.H.; Kats, K.P.; Hochstenbach, R.; Pasterkamp, G.; et al. TGF-beta1 induces efficient differentiation of human cardiomyocyte progenitor cells into functional cardiomyocytes in vitro. *Stem. Cell Res.* **2007**, *1*, 138–149. [CrossRef] [PubMed]
12. Huang, X.; Le, Q.T.; Giaccia, A.J. MiR-210--micromanager of the hypoxia pathway. *Trends Mol. Med.* **2010**, *16*, 230–237. [CrossRef]
13. Kiriyama, M.; Kobayashi, Y.; Saito, M.; Ishikawa, F.; Yonehara, S. Interaction of FLASH with arsenite resistance protein 2 is involved in cell cycle progression at S phase. *Mol. Cell Biol.* **2009**, *29*, 4729–4741. [CrossRef] [PubMed]

14. Alm-Kristiansen, A.H.; Saether, T.; Matre, V.; Gilfillan, S.; Dahle, O.; Gabrielsen, O.S. FLASH acts as a co-activator of the transcription factor c-Myb and localizes to active RNA polymerase II foci. *Oncogene* **2008**, *27*, 4644–4656. [CrossRef]
15. Imai, Y.; Kimura, T.; Murakami, A.; Yajima, N.; Sakamaki, K.; Yonehara, S. The CED-4-homologous protein FLASH is involved in Fas-mediated activation of caspase-8 during apoptosis. *Nature* **1999**, *398*, 777–785. [CrossRef] [PubMed]
16. Li, J.; Lin, Q.; Shao, X.; Li, S.; Zhu, X.; Wu, J.; Mou, S.; Gu, L.; Wang, Q.; Zhang, M.; et al. HIF1alpha-BNIP3-mediated mitophagy protects against renal fibrosis by decreasing ROS and inhibiting activation of the NLRP3 inflammasome. *Cell Death Dis.* **2023**, *14*, 200. [CrossRef]
17. Smith, R.R.; Barile, L.; Cho, H.C.; Leppo, M.K.; Hare, J.M.; Messina, E.; Giacomello, A.; Abraham, M.R.; Marban, E. Regenerative potential of cardiosphere-derived cells expanded from percutaneous endomyocardial biopsy specimens. *Circulation* **2007**, *115*, 896–908. [CrossRef]
18. Claycomb, W.C.; Lanson, N.A., Jr.; Stallworth, B.S.; Egeland, D.B.; Delcarpio, J.B.; Bahinski, A.; Izzo, N.J., Jr. HL-1 cells: A cardiac muscle cell line that contracts and retains phenotypic characteristics of the adult cardiomyocyte. *Proc. Natl. Acad. Sci. USA* **1998**, *95*, 2979–2984. [CrossRef]
19. Livak, K.J.; Schmittgen, T.D. Analysis of relative gene expression data using real-time quantitative PCR and the 2(-Delta Delta C(T)) Method. *Methods* **2001**, *25*, 402–408. [CrossRef]
20. Bolte, S.; Cordelieres, F.P. A guided tour into subcellular colocalization analysis in light microscopy. *J. Microsc.* **2006**, *224*, 213–232. [CrossRef]
21. Gavet, O.; Pines, J. Progressive activation of CyclinB1-Cdk1 coordinates entry to mitosis. *Dev. Cell* **2010**, *18*, 533–543. [CrossRef] [PubMed]
22. Collins, C.L.; Bode, B.P.; Souba, W.W.; Abcouwer, S.F. Multiwell 14CO2-capture assay for evaluation of substrate oxidation rates of cells in culture. *Biotechniques* **1998**, *24*, 803–808. [CrossRef]
23. Esteban-Martinez, L.; Sierra-Filardi, E.; Boya, P. Mitophagy, metabolism, and cell fate. *Mol. Cell Oncol.* **2017**, *4*, e1353854. [CrossRef]
24. McWilliams, T.G.; Prescott, A.R.; Montava-Garriga, L.; Ball, G.; Singh, F.; Barini, E.; Muqit, M.M.K.; Brooks, S.P.; Ganley, I.G. Basal Mitophagy Occurs Independently of PINK1 in Mouse Tissues of High Metabolic Demand. *Cell Metab* **2018**, *27*, 439–449.e435. [CrossRef]
25. Kelly, T.J.; Souza, A.L.; Clish, C.B.; Puigserver, P. A hypoxia-induced positive feedback loop promotes hypoxia-inducible factor 1alpha stability through miR-210 suppression of glycerol-3-phosphate dehydrogenase 1-like. *Mol. Cell. Biol.* **2011**, *31*, 2696–2706. [CrossRef] [PubMed]
26. Kim, J.W.; Tchernyshyov, I.; Semenza, G.L.; Dang, C.V. HIF-1-mediated expression of pyruvate dehydrogenase kinase: A metabolic switch required for cellular adaptation to hypoxia. *Cell Metab.* **2006**, *3*, 177–185. [CrossRef]
27. Papandreou, I.; Cairns, R.A.; Fontana, L.; Lim, A.L.; Denko, N.C. HIF-1 mediates adaptation to hypoxia by actively downregulating mitochondrial oxygen consumption. *Cell Metab.* **2006**, *3*, 187–197. [CrossRef]
28. Favaro, E.; Ramachandran, A.; McCormick, R.; Gee, H.; Blancher, C.; Crosby, M.; Devlin, C.; Blick, C.; Buffa, F.; Li, J.L.; et al. MicroRNA-210 regulates mitochondrial free radical response to hypoxia and krebs cycle in cancer cells by targeting iron sulfur cluster protein ISCU. *PLoS ONE* **2010**, *5*, e10345. [CrossRef] [PubMed]
29. Kwon, J.J.; Factora, T.D.; Dey, S.; Kota, J. A Systematic Review of miR-29 in Cancer. *Mol. Ther. Oncolytics* **2019**, *12*, 173–194. [CrossRef]
30. Cao, R.Y.; Li, Q.; Miao, Y.; Zhang, Y.; Yuan, W.; Fan, L.; Liu, G.; Mi, Q.; Yang, J. The Emerging Role of MicroRNA-155 in Cardiovascular Diseases. *Biomed. Res. Int.* **2016**, *2016*, 9869208. [CrossRef]
31. Si, W.; Shen, J.; Zheng, H.; Fan, W. The role and mechanisms of action of microRNAs in cancer drug resistance. *Clin. Epigenetics* **2019**, *11*, 25. [CrossRef] [PubMed]
32. Yang, C.; Tabatabaei, S.N.; Ruan, X.; Hardy, P. The Dual Regulatory Role of MiR-181a in Breast Cancer. *Cell Physiol. Biochem.* **2017**, *44*, 843–856. [CrossRef] [PubMed]
33. Tsang, J.; Zhu, J.; van Oudenaarden, A. MicroRNA-mediated feedback and feedforward loops are recurrent network motifs in mammals. *Mol. Cell* **2007**, *26*, 753–767. [CrossRef]
34. Seoudi, A.M.; Lashine, Y.A.; Abdelaziz, A.I. MicroRNA-181a—A tale of discrepancies. *Expert. Rev. Mol. Med.* **2012**, *14*, e5. [CrossRef] [PubMed]
35. Tagscherer, K.E.; Fassl, A.; Sinkovic, T.; Richter, J.; Schecher, S.; Macher-Goeppinger, S.; Roth, W. MicroRNA-210 induces apoptosis in colorectal cancer via induction of reactive oxygen. *Cancer Cell Int.* **2016**, *16*, 42. [CrossRef]
36. Kim, H.W.; Haider, H.K.; Jiang, S.; Ashraf, M. Ischemic preconditioning augments survival of stem cells via miR-210 expression by targeting caspase-8-associated protein 2. *J. Biol. Chem.* **2009**, *284*, 33161–33168. [CrossRef]
37. Hu, S.; Huang, M.; Li, Z.; Jia, F.; Ghosh, Z.; Lijkwan, M.A.; Fasanaro, P.; Sun, N.; Wang, X.; Martelli, F.; et al. MicroRNA-210 as a novel therapy for treatment of ischemic heart disease. *Circulation* **2010**, *122*, S124–S131. [CrossRef]

38. Arif, M.; Pandey, R.; Alam, P.; Jiang, S.; Sadayappan, S.; Paul, A.; Ahmed, R.P.H. MicroRNA-210-mediated proliferation, survival, and angiogenesis promote cardiac repair post myocardial infarction in rodents. *J. Mol. Med.* **2017**, *95*, 1369–1385. [CrossRef]
39. Barile, L.; Lionetti, V.; Cervio, E.; Matteucci, M.; Gherghiceanu, M.; Popescu, L.M.; Torre, T.; Siclari, F.; Moccetti, T.; Vassalli, G. Extracellular vesicles from human cardiac progenitor cells inhibit cardiomyocyte apoptosis and improve cardiac function after myocardial infarction. *Cardiovasc. Res.* **2014**, *103*, 530–541. [CrossRef]
40. Gray, W.D.; French, K.M.; Ghosh-Choudhary, S.; Maxwell, J.T.; Brown, M.E.; Platt, M.O.; Searles, C.D.; Davis, M.E. Identification of therapeutic covariant microRNA clusters in hypoxia-treated cardiac progenitor cell exosomes using systems biology. *Circ. Res.* **2015**, *116*, 255–263. [CrossRef]
41. Ma, X.; Wang, J.; Li, J.; Ma, C.; Chen, S.; Lei, W.; Yang, Y.; Liu, S.; Bihl, J.; Chen, C. Loading MiR-210 in Endothelial Progenitor Cells Derived Exosomes Boosts Their Beneficial Effects on Hypoxia/Reoxygeneation-Injured Human Endothelial Cells via Protecting Mitochondrial Function. *Cell Physiol. Biochem.* **2018**, *46*, 664–675. [CrossRef] [PubMed]
42. Lakhani, S.A.; Masud, A.; Kuida, K.; Porter, G.A., Jr.; Booth, C.J.; Mehal, W.Z.; Inayat, I.; Flavell, R.A. Caspases 3 and 7: Key mediators of mitochondrial events of apoptosis. *Science* **2006**, *311*, 847–851. [CrossRef] [PubMed]
43. Montava-Garriga, L.; Ganley, I.G. Outstanding Questions in Mitophagy: What We Do and Do Not Know. *J. Mol. Biol.* **2020**, *432*, 206–230. [CrossRef]
44. Rodger, C.E.; McWilliams, T.G.; Ganley, I.G. Mammalian mitophagy—From in vitro molecules to in vivo models. *FEBS J.* **2018**, *285*, 1185–1202. [CrossRef] [PubMed]
45. Folmes, C.D.; Nelson, T.J.; Martinez-Fernandez, A.; Arrell, D.K.; Lindor, J.Z.; Dzeja, P.P.; Ikeda, Y.; Perez-Terzic, C.; Terzic, A. Somatic oxidative bioenergetics transitions into pluripotency-dependent glycolysis to facilitate nuclear reprogramming. *Cell Metab.* **2011**, *14*, 264–271. [CrossRef]
46. Zhong, X.; Cui, P.; Cai, Y.; Wang, L.; He, X.; Long, P.; Lu, K.; Yan, R.; Zhang, Y.; Pan, X.; et al. Mitochondrial Dynamics Is Critical for the Full Pluripotency and Embryonic Developmental Potential of Pluripotent Stem Cells. *Cell Metab.* **2019**, *29*, 979–992.e974. [CrossRef]
47. Xiang, G.; Yang, L.; Long, Q.; Chen, K.; Tang, H.; Wu, Y.; Liu, Z.; Zhou, Y.; Qi, J.; Zheng, L.; et al. BNIP3L-dependent mitophagy accounts for mitochondrial clearance during 3 factors-induced somatic cell reprogramming. *Autophagy* **2017**, *13*, 1543–1555. [CrossRef]
48. Chen, Z.; Li, Y.; Zhang, H.; Huang, P.; Luthra, R. Hypoxia-regulated microRNA-210 modulates mitochondrial function and decreases ISCU and COX10 expression. *Oncogene* **2010**, *29*, 4362–4368. [CrossRef]
49. Qiao, A.; Khechaduri, A.; Kannan Mutharasan, R.; Wu, R.; Nagpal, V.; Ardehali, H. MicroRNA-210 decreases heme levels by targeting ferrochelatase in cardiomyocytes. *J. Am. Heart Assoc.* **2013**, *2*, e000121. [CrossRef]
50. Fasanaro, P.; Greco, S.; Lorenzi, M.; Pescatori, M.; Brioschi, M.; Kulshreshtha, R.; Banfi, C.; Stubbs, A.; Calin, G.A.; Ivan, M.; et al. An integrated approach for experimental target identification of hypoxia-induced miR-210. *J. Biol. Chem.* **2009**, *284*, 35134–35143. [CrossRef]
51. Chan, S.Y.; Zhang, Y.Y.; Hemann, C.; Mahoney, C.E.; Zweier, J.L.; Loscalzo, J. MicroRNA-210 controls mitochondrial metabolism during hypoxia by repressing the iron-sulfur cluster assembly proteins ISCU1/2. *Cell Metab.* **2009**, *10*, 273–284. [CrossRef] [PubMed]
52. Fong, G.H.; Takeda, K. Role and regulation of prolyl hydroxylase domain proteins. *Cell Death Differ.* **2008**, *15*, 635–641. [CrossRef]
53. D'Angelo, G.; Duplan, E.; Boyer, N.; Vigne, P.; Frelin, C. Hypoxia up-regulates prolyl hydroxylase activity: A feedback mechanism that limits HIF-1 responses during reoxygenation. *J. Biol. Chem.* **2003**, *278*, 38183–38187. [CrossRef] [PubMed]
54. Majmundar, A.J.; Wong, W.J.; Simon, M.C. Hypoxia-inducible factors and the response to hypoxic stress. *Mol. Cell* **2010**, *40*, 294–309. [CrossRef]
55. Marxsen, J.H.; Stengel, P.; Doege, K.; Heikkinen, P.; Jokilehto, T.; Wagner, T.; Jelkmann, W.; Jaakkola, P.; Metzen, E. Hypoxia-inducible factor-1 (HIF-1) promotes its degradation by induction of HIF-alpha-prolyl-4-hydroxylases. *Biochem. J.* **2004**, *381*, 761–767. [CrossRef]
56. Sentelle, R.D.; Senkal, C.E.; Jiang, W.; Ponnusamy, S.; Gencer, S.; Selvam, S.P.; Ramshesh, V.K.; Peterson, Y.K.; Lemasters, J.J.; Szulc, Z.M.; et al. Ceramide targets autophagosomes to mitochondria and induces lethal mitophagy. *Nat. Chem. Biol.* **2012**, *8*, 831–838. [CrossRef]
57. Yao, C.H.; Wang, R.; Wang, Y.; Kung, C.P.; Weber, J.D.; Patti, G.J. Mitochondrial fusion supports increased oxidative phosphorylation during cell proliferation. *Elife* **2019**, *8*, e41351. [CrossRef]
58. Rambold, A.S.; Kostelecky, B.; Elia, N.; Lippincott-Schwartz, J. Tubular network formation protects mitochondria from autophagosomal degradation during nutrient starvation. *Proc. Natl. Acad. Sci. USA* **2011**, *108*, 10190–10195. [CrossRef] [PubMed]
59. Song, W.; Wang, H.; Wu, Q. Atrial natriuretic peptide in cardiovascular biology and disease (NPPA). *Gene* **2015**, *569*, 1–6. [CrossRef]
60. Shi, Y.; Chang, M.; Wang, F.; Ouyang, X.; Jia, Y.; Du, H. Role and mechanism of hypoxia-inducible factor-1 in cell growth and apoptosis of breast cancer cell line MDA-MB-231. *Oncol. Lett.* **2010**, *1*, 657–662. [CrossRef]

61. Thomas, R.; Kim, M.H. HIF-1 alpha: A key survival factor for serum-deprived prostate cancer cells. *Prostate* **2008**, *68*, 1405–1415. [CrossRef] [PubMed]
62. Bruick, R.K. Expression of the gene encoding the proapoptotic Nip3 protein is induced by hypoxia. *Proc. Natl. Acad. Sci. USA* **2000**, *97*, 9082–9087. [CrossRef] [PubMed]
63. Guo, K.; Searfoss, G.; Krolikowski, D.; Pagnoni, M.; Franks, C.; Clark, K.; Yu, K.T.; Jaye, M.; Ivashchenko, Y. Hypoxia induces the expression of the pro-apoptotic gene BNIP3. *Cell Death Dif.* **2001**, *8*, 367–376. [CrossRef] [PubMed]
64. Zhang, J.; Ney, P.A. Role of BNIP3 and NIX in cell death, autophagy, and mitophagy. *Cell Death Differ.* **2009**, *16*, 939–946. [CrossRef]
65. Moriyama, M.; Moriyama, H.; Uda, J.; Kubo, H.; Nakajima, Y.; Goto, A.; Morita, T.; Hayakawa, T. BNIP3 upregulation via stimulation of ERK and JNK activity is required for the protection of keratinocytes from UVB-induced apoptosis. *Cell Death Dis.* **2017**, *8*, e2576. [CrossRef]
66. Burton, T.R.; Gibson, S.B. The role of Bcl-2 family member BNIP3 in cell death and disease: NIPping at the heels of cell death. *Cell Death Differ.* **2009**, *16*, 515–523. [CrossRef]
67. Kim, H.W.; Jiang, S.; Ashraf, M.; Haider, K.H. Stem cell-based delivery of Hypoxamir-210 to the infarcted heart: Implications on stem cell survival and preservation of infarcted heart function. *J. Mol. Med.* **2012**, *90*, 997–1010. [CrossRef]
68. Kim, K.L.; Seo, S.; Kim, J.T.; Kim, J.; Kim, W.; Yeo, Y.; Sung, J.H.; Park, S.G.; Suh, W. SCF (Stem Cell Factor) and cKIT Modulate Pathological Ocular Neovascularization. *Arterioscler. Thromb. Vasc. Biol.* **2019**, *39*, 2120–2131. [CrossRef]
69. Han, Z.B.; Ren, H.; Zhao, H.; Chi, Y.; Chen, K.; Zhou, B.; Liu, Y.J.; Zhang, L.; Xu, B.; Liu, B.; et al. Hypoxia-inducible factor (HIF)-1 alpha directly enhances the transcriptional activity of stem cell factor (SCF) in response to hypoxia and epidermal growth factor (EGF). *Carcinogenesis* **2008**, *29*, 1853–1861. [CrossRef]
70. Wang, X.; Dong, J.; Jia, L.; Zhao, T.; Lang, M.; Li, Z.; Lan, C.; Li, X.; Hao, J.; Wang, H.; et al. HIF-2-dependent expression of stem cell factor promotes metastasis in hepatocellular carcinoma. *Cancer Lett.* **2017**, *393*, 113–124. [CrossRef]
71. Matsui, J.; Wakabayashi, T.; Asada, M.; Yoshimatsu, K.; Okada, M. Stem cell factor/c-kit signaling promotes the survival, migration, and capillary tube formation of human umbilical vein endothelial cells. *J. Biol. Chem.* **2004**, *279*, 18600–18607. [CrossRef] [PubMed]
72. Xiang, F.L.; Lu, X.; Hammoud, L.; Zhu, P.; Chidiac, P.; Robbins, J.; Feng, Q. Cardiomyocyte-specific overexpression of human stem cell factor improves cardiac function and survival after myocardial infarction in mice. *Circulation* **2009**, *120*, 1065–1074. [CrossRef] [PubMed]
73. Bach, L.A. Endothelial cells and the IGF system. *J. Mol. Endocrinol.* **2015**, *54*, R1–R13. [CrossRef]
74. Ellison, G.M.; Torella, D.; Dellegrottaglie, S.; Perez-Martinez, C.; Perez de Prado, A.; Vicinanza, C.; Purushothaman, S.; Galuppo, V.; Iaconetti, C.; Waring, C.D.; et al. Endogenous cardiac stem cell activation by insulin-like growth factor-1/hepatocyte growth factor intracoronary injection fosters survival and regeneration of the infarcted pig heart. *J. Am. Coll Cardiol.* **2011**, *58*, 977–986. [CrossRef] [PubMed]
75. Fasanaro, P.; D'Alessandra, Y.; Di Stefano, V.; Melchionna, R.; Romani, S.; Pompilio, G.; Capogrossi, M.C.; Martelli, F. MicroRNA-210 modulates endothelial cell response to hypoxia and inhibits the receptor tyrosine kinase ligand Ephrin-A3. *J. Biol. Chem.* **2008**, *283*, 15878–15883. [CrossRef]
76. Lou, Y.L.; Guo, F.; Liu, F.; Gao, F.L.; Zhang, P.Q.; Niu, X.; Guo, S.C.; Yin, J.H.; Wang, Y.; Deng, Z.F. miR-210 activates notch signaling pathway in angiogenesis induced by cerebral ischemia. *Mol. Cell Biochem.* **2012**, *370*, 45–51. [CrossRef] [PubMed]
77. Chimenti, I.; Smith, R.R.; Li, T.S.; Gerstenblith, G.; Messina, E.; Giacomello, A.; Marban, E. Relative roles of direct regeneration versus paracrine effects of human cardiosphere-derived cells transplanted into infarcted mice. *Circ. Res.* **2010**, *106*, 971–980. [CrossRef]
78. Hsiao, S.T.; Lokmic, Z.; Peshavariya, H.; Abberton, K.M.; Dusting, G.J.; Lim, S.Y.; Dilley, R.J. Hypoxic conditioning enhances the angiogenic paracrine activity of human adipose-derived stem cells. *Stem. Cells Dev.* **2013**, *22*, 1614–1623. [CrossRef]
79. Fierro, F.A.; O'Neal, A.J.; Beegle, J.R.; Chavez, M.N.; Peavy, T.R.; Isseroff, R.R.; Egana, J.T. Hypoxic pre-conditioning increases the infiltration of endothelial cells into scaffolds for dermal regeneration pre-seeded with mesenchymal stem cells. *Front. Cell Dev. Biol.* **2015**, *3*, 68. [CrossRef]
80. Bader, A.M.; Klose, K.; Bieback, K.; Korinth, D.; Schneider, M.; Seifert, M.; Choi, Y.H.; Kurtz, A.; Falk, V.; Stamm, C. Hypoxic Preconditioning Increases Survival and Pro-Angiogenic Capacity of Human Cord Blood Mesenchymal Stromal Cells In Vitro. *PLoS ONE* **2015**, *10*, e0138477. [CrossRef]
81. Tan, S.C.; Gomes, R.S.; Yeoh, K.K.; Perbellini, F.; Malandraki-Miller, S.; Ambrose, L.; Heather, L.C.; Faggian, G.; Schofield, C.J.; Davies, K.E.; et al. Preconditioning of Cardiosphere-Derived Cells With Hypoxia or Prolyl-4-Hydroxylase Inhibitors Increases Stemness and Decreases Reliance on Oxidative Metabolism. *Cell Transplant.* **2016**, *25*, 35–53. [CrossRef] [PubMed]
82. Park, C.Y.; Choi, S.C.; Kim, J.H.; Choi, J.H.; Joo, H.J.; Hong, S.J.; Lim, D.S. Cardiac Stem Cell Secretome Protects Cardiomyocytes from Hypoxic Injury Partly via Monocyte Chemotactic Protein-1-Dependent Mechanism. *Int. J. Mol. Sci.* **2016**, *17*, 800. [CrossRef] [PubMed]

83. Levy, J.; Cacheux, W.; Bara, M.A.; L'Hermitte, A.; Lepage, P.; Fraudeau, M.; Trentesaux, C.; Lemarchand, J.; Durand, A.; Crain, A.M.; et al. Intestinal inhibition of Atg7 prevents tumour initiation through a microbiome-influenced immune response and suppresses tumour growth. *Nat. Cell Biol.* **2015**, *17*, 1062–1073. [CrossRef] [PubMed]
84. Ghosh, M.C.; Zhang, D.L.; Jeong, S.Y.; Kovtunovych, G.; Ollivierre-Wilson, H.; Noguchi, A.; Tu, T.; Senecal, T.; Robinson, G.; Crooks, D.R.; et al. Deletion of iron regulatory protein 1 causes polycythemia and pulmonary hypertension in mice through translational derepression of HIF2alpha. *Cell Metab.* **2013**, *17*, 271–281. [CrossRef]
85. Chung, E.; Joiner, H.E.; Skelton, T.; Looten, K.D.; Manczak, M.; Reddy, P.H. Maternal exercise upregulates mitochondrial gene expression and increases enzyme activity of fetal mouse hearts. *Physiol. Rep.* **2017**, *5*, e13184. [CrossRef]
86. Ha, S.D.; Ng, D.; Lamothe, J.; Valvano, M.A.; Han, J.; Kim, S.O. Mitochondrial proteins Bnip3 and Bnip3L are involved in anthrax lethal toxin-induced macrophage cell death. *J. Biol. Chem.* **2007**, *282*, 26275–26283. [CrossRef]
87. Nytko, K.J.; Maeda, N.; Schlafli, P.; Spielmann, P.; Wenger, R.H.; Stiehl, D.P. Vitamin C is dispensable for oxygen sensing in vivo. *Blood* **2011**, *117*, 5485–5493. [CrossRef]
88. Audesse, A.J.; Dhakal, S.; Hassell, L.A.; Gardell, Z.; Nemtsova, Y.; Webb, A.E. FOXO3 directly regulates an autophagy network to functionally regulate proteostasis in adult neural stem cells. *PLoS Genet.* **2019**, *15*, e1008097. [CrossRef]
89. Gold, W.A.; Williamson, S.L.; Kaur, S.; Hargreaves, I.P.; Land, J.M.; Pelka, G.J.; Tam, P.P.; Christodoulou, J. Mitochondrial dysfunction in the skeletal muscle of a mouse model of Rett syndrome (RTT): Implications for the disease phenotype. *Mitochondrion* **2014**, *15*, 10–17. [CrossRef]